Stabilization of electrons on Ar^{q+} ions after slow collisions with C_{60}

A. Langereis and J. Jensen
Manne Siegbahn Laboratory, Frescativägen 24, S-104 05 Stockholm, Sweden

A. Fardi, K. Haghighat, H. T. Schmidt, S. H. Schwartz, H. Zettergren, and H. Cederquist
Physics Department, Stockholm University, Frescativägen 24, S-104 05 Stockholm, Sweden

(Received 21 December 2000; published 17 May 2001)

We discuss hollow atom formation and stabilization of electrons on Ar^{q+} following $Ar^{q+}+C_{60} \rightarrow Ar^{(q-s)+}+\cdots$ collisions at $3.3q$ keV ($q=4-18$). The experimental information consists of the final projectile charge-state distributions f_q^s, i.e., the relative distributions of the number of stabilized electrons, s, and the corresponding mean values $\langle s\rangle=\Sigma_{s=1}^{q} s f_q^s$ as functions of q. We use the classical over-the-barrier model to deduce sequences of effective principal quantum numbers and find that the hollow atom formation is completed $3-4a_0$ above the surface of the C_{60} cage for all q. For $q\leqslant 8$ (filled L shells), the last electrons are transferred from delocalized outer C_{60} orbitals directly to the projectile M shell (side-feeding), while several intermediate shells are left open for larger q leading to further electron transfer at intermediate distances and simultaneous electron emission from higher projectile shells. At still closer distances, localized carbon K-shell electrons are transferred directly to the argon L ($q=10$ and 11) and M shells ($q\geqslant 12$). The direct transfer to the L shell of Ar^{10+} and Ar^{11+} is manifested as significant enhancements of $\langle s\rangle$ for $q=10$ and $q=11$.

DOI: 10.1103/PhysRevA.63.062725 PACS number(s): 34.70.+e

I. INTRODUCTION

The interactions between slow highly charged ions and atoms, molecules, clusters, microcapillaries, and solid surfaces have been studied extensively during the past few decades (for reviews, see [1,2]). One of the common main characteristics of such interactions is electron transfer from the target to highly excited projectile states. Hollow atoms and ions are thus formed with features that depend on the impact parameter, the projectile charge q, and the electronic properties of the target. Clusters, microcapillaries, and surfaces have large amounts of loosely bound electrons yielding efficient population of such exotic states, but it is only the former two [3–7] that offer possibilities to study free hollow atoms at longer times after their creations.

Hollow atoms formed along trajectories towards flat surfaces are destroyed in close interactions with surface and bulk atoms. The number of electrons leaving the surface may be very large and is often greater than q [8,9], especially when there are strong contributions from below-surface processes [10]. A further important feature of the inevitable close collisions is the efficient, q-independent, neutralization in grazing interactions with metal [11,12] and insulator [13,14] surfaces. This means that inner-shell vacancies are filled during the very short collision time of typically 10 fs. For years this seemed to be hard to reconcile with the anticipated much longer Auger and radiative relaxation times for hollow atoms, often referred to as the time-bottleneck problem (see, e.g., [15]). However, Winecki *et al.* [16–18] have shown that very fast above-the-surface neutralization of Ar^{q+} on graphite may be accounted for through direct transfer to the projectile M-shell and following fast LMM Auger transitions. Such over-the-barrier transfers at close distances bypass time-consuming relaxation cascades, and in the field of ion-surface collisions they are often referred to as side-feeding processes [19]. In this work, we will discuss the importance of related processes and possible time-bottleneck limitations for electron transfer and stabilization in $Ar^{q+}-C_{60}$ collisions. Right from the onset we would like to stress though that interactions between highly charged ions and C_{60} are dominated by processes at large impact parameters in which the molecule may be viewed as a pointlike (atomic) target [20].

We have thus investigated electron transfer and the subsequent stabilization of electrons on the projectile in

$$Ar^{q+}+C_{60} \rightarrow Ar^{(q-s)+}+{C_{60}}^{r+}+(r-s)e^{-} \tag{1}$$

collisions at $3.3q$ keV with $q=4$, 6, and 8–18. We define the final projectile charge-state distributions, f_q^s, as

$$f_q^s=\frac{\sigma_q^s}{\sum_{s=1}^{q}\sigma_q^s}, \tag{2}$$

where σ_q^s is the absolute cross section for stabilization of s electrons. The mean numbers of stabilized electrons are then given by

$$\langle s\rangle=\sum_{s=1}^{q} s f_q^s. \tag{3}$$

Most of the collisions (1) occur at large distances and only a limited amount of electrons are removed from the target and only one or a few are stabilized on the projectile. A smaller part, however, shows surfacelike features such as, for example, strong electron emission. This very astonishing effect—there is nothing below the surface in C_{60}—was first reported by Martin *et al.* [21] and so far no fully convincing explanation has been offered.

In Sec. II, we give a brief description of the experimental technique and we present the results in Sec. III. The f_q^s data fall in two main groups, $f_{q,\mathrm{high}}^s$ and $f_{q,\mathrm{low}}^s$, within each of which the q dependences are very weak. This finding is discussed in Sec. IV and may be traced back to the relaxation of multiply excited states and the weak q dependence for the relative target ionization cross sections,

$$f_q^r = \frac{\sigma_q^r}{\sum_{r=1}^{q} \sigma_q^r}, \tag{4}$$

where σ_q^r is the cross section for removing r electrons from the target.

Electron transfer is described as sequences of classical over-the-barrier processes yielding corresponding sequences of effective principal quantum numbers for the projectile capture states. We find that the last transferred electrons in the hollow atom formation populate states close to the projectile core for lower q, while the higher-q projectiles may be fully neutralized leaving several intermediate shells empty. The M shell is thus populated directly from outer C_{60} orbitals in over-the-barrier processes for $q \leqslant 8$. For higher q, resonant transfers between the carbon K and the argon L ($q=10$ and 11) are very effective in analogy with the reverse process (argon L-shell vacancy production in atomic C^{6+}-Ar collisions) reported by deNijs *et al.* [22]. For $q \geqslant 12$, the carbon K-shell electrons appear to be transferred to the projectile M shell.

The inner-shell transfer distances are well within the distance from the C_{60} surface ($3-4a_0$) where the hollow atom formation is completed. The possibility of filling vacant intermediate shells after forming the hollow atom suggests a mechanism for dissipating many electrons during the close part of the collision. This interaction time is too short (subfemtoseconds) to allow for filling of the innermost open projectile shells via inner-shell Auger processes as in ion-surface collisions.

II. EXPERIMENT

The experimental procedure has been discussed in detail earlier [5,20]. Briefly, the argon ions were produced by the cryogenic electron beam ion source at the Manne Siegbahn Laboratory, Stockholm University. The ions had energies of $3.3q$ keV and their mass-to-charge ratios were selected with a double focusing analyzing magnet. Behind the magnet, the beam was collimated before it entered a cylinder containing a vapor of C_{60} from a 99.9% pure powder (Hoechst). The cylinder was temperature-stabilized within $\pm 1°$ and set to values (in the interval 410–420 °C) such that the total charge-exchange yields were below 10% for all q when the charge-state fractions, f_q^s, were recorded. This made corrections for double and background collisions small but not negligible [20]. The charge exchange with the background gas was measured at cell temperatures of 300 and 350 °C. After the interaction region, the $Ar^{(q-s)+}$ ions passed a 300-mm-long field-free region. The final projectile charge states ($q-s$) were selected by means of a 180 ° cylindrical energy analyzer as shown in Fig. 1. Alternatively, short deflector plates were used to disperse the different ($q-s$) beams on a position-sensitive detector. This second setup also allowed for measuring the cross sections for projectile neutralization [5].

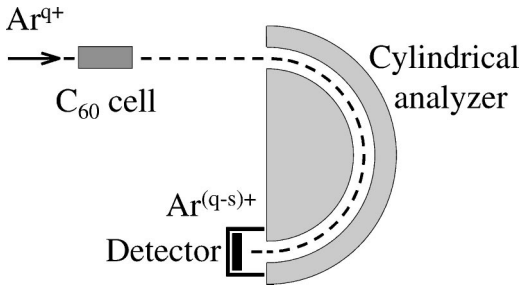

FIG. 1. A schematic of the experimental setup used to measure absolute cross sections, σ_q^s, final charge-state distributions, f_q^s, and mean numbers of stabilized electrons, $\langle s \rangle_{C60}$, in $3.3q$ keV $Ar^{q+} - C_{60} \rightarrow Ar^{(q-s)+} + \cdots$ collisions.

The f_q^s distributions were established by switching between the primary beam of charge q and all the different charge-exchange components, defined by s, during short times. This procedure was repeated many times in order to arrive at mean ratios $N(q-s)/N(q)$, where $N(q-s)$ and $N(q)$ were the number of ions of charges $q-s$ and q, respectively, that were registered during a certain preset time and at a well-defined target density (temperature) [20]. We determined the absolute cross-section scale using the vapor pressure by Abrefah *et al.* [23]. This choice has recently been motivated in detail by Schwartz *et al.* [20] and Larsson *et al.* [24].

III. RESULTS

The measured absolute cross sections for stabilizing s electrons in $Ar^{q+} - C_{60}$ collisions are shown in Fig. 2. We note that the cross sections σ_q^s increase with q for $s=1,2,3$, are roughly independent of q for $s=4$, and are strongly reduced above $q=10$ for $s=5$ and 6.

The experimental f_q^s distributions, deduced from Eq. (2), are shown in Fig. 3. For lower s, they both decrease monotonically with s. For $s \geqslant 5$, the distributions fall in the two groups $f_{q,\mathrm{low}}^s$ ($q \leqslant 10$) and $f_{q,\mathrm{high}}^s$ ($q \geqslant 12$) (left and right side of Fig. 3, respectively). The $f_{q,\mathrm{high}}^s$ fractions are very small (mostly $<0.1\%$) for $s>5$ while the $f_{q,\mathrm{low}}^s$ fractions have a second maximum for $s \geqslant 5$. We note that the $f_{q,\mathrm{low}}^s$ and $f_{q,\mathrm{high}}^s$ distributions are almost independent of q within each group. Further, for $s \leqslant 4$ there are only small differences even between the two groups.

In Fig. 4, we show in detail the parts of the $f_{q,\mathrm{low}}^s$ and $f_{q,\mathrm{high}}^s$ distributions that lie below 10% in order to clearly expose the differences for $s \geqslant 5$

The $f_{q=11}^s$ distribution lies between $f_{q,\mathrm{low}}^s$ and $f_{q,\mathrm{high}}^s$. Note also that the $f_{q,\mathrm{low}}^{s=5}$ value for $q=6$ and the $f_{q,\mathrm{low}}^{s=7}$ value for $q=8$ fall outside the general trend for $f_{q,\mathrm{low}}^s$.

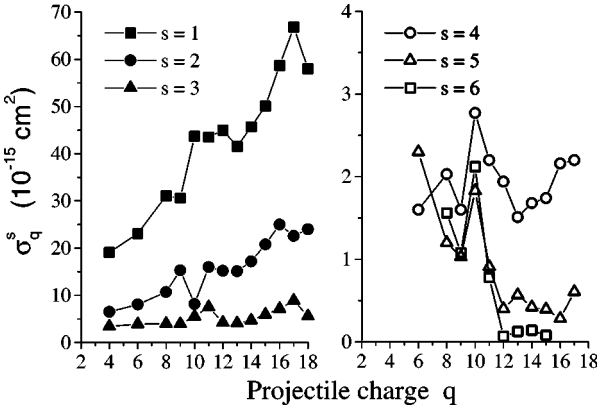

FIG. 2. The total cross sections σ_q^s for stabilizing s electrons as functions of q in $3.3q$ keV Ar^{q+}-C_{60} collisions. Note the difference in σ_q^s scales for the left and the right figures. The absolute cross-section scale is set by the vapor pressure by Abrefah *et al.* [23] giving an estimated uncertainty of $\pm 30\%$ [20]. The statistical uncertainties are much smaller than this (typically a few percent). The lines have been drawn to guide the eye.

IV. DISCUSSION

The $f_{q,\mathrm{low}}^s$ and $f_{q,\mathrm{high}}^s$ distributions for the C_{60} target are similar for low numbers of stabilized electrons ($s=1-4$). In this region of s, they are also similar to the projectile charge-state distributions for Ar^{q+}-Ar collisions from Ali *et al.* [25]. The latter similarity shows that $Ar^{q+}-C_{60}$ interactions yielding $s=1-4$ are dominated by large impact parameter collisions in which the geometrical dimensions of the target are relatively unimportant. These processes account for larger parts (more than 80%) of the total charge-exchange cross sections and thus $Ar^{q+}-C_{60}$ collisions are mostly ''atom-like.''

In the following, we will first give a short description of the over-the-barrier model used to calculate critical distances for electron transfer and effective quantum numbers for the capture states. Then, we will discuss the formation of hollow ions and atoms and compare electron transfer and stabilization following low-velocity $Ar^{q+}-C_{60}$, Ar^{q+}-atom (He [26,27] and Ar [25]), and Ar^{q+}-graphite surface [16–18] collisions.

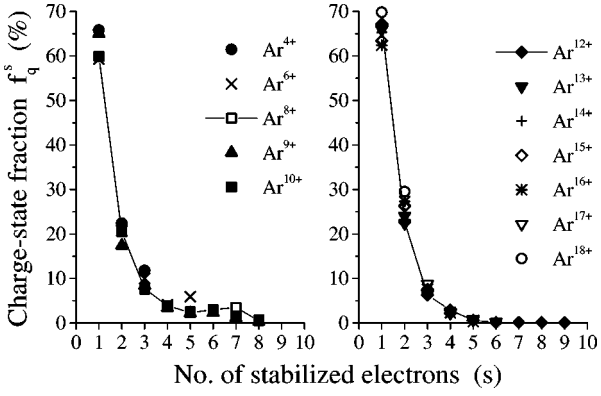

FIG. 3. Experimental final projectile charge-state fractions f_q^s as functions of the number of electrons, s, stabilized on $3.3q$ keV Ar^{q+} projectiles after collisions with C_{60}. The lines are to guide the eye.

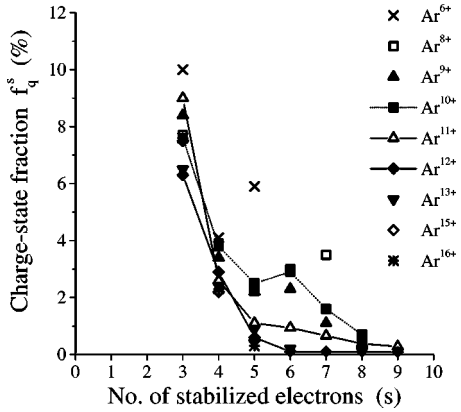

FIG. 4. The $f_{q,\mathrm{low}}^s$ and $f_{q,\mathrm{high}}^s$ distributions with an expanded vertical scale. The lines trace the f_q^s distributions for $q=10$, 11, and 12.

A. Modeling electron transfer from C_{60}

Most versions of the over-the-barrier model for ion-C_{60} collisions [3–5,28] are built on metal-sphere descriptions of the C_{60} molecule [3–5] and here we adopt this picture. We set the sphere radius to $a=7.2\ a_0$ by means of the experimental values for the sequence of ionization potentials I_r [29–31] and the polarizability α [32] of C_{60}. This yields $a=7.2\pm 0.1a_0$ using classical electrostatics for which $I_r=(r+1)/a$ and $\alpha=a^3$. The former gives $I_r=3.76(r+1)$ eV, which will be used throughout this work.

The critical over-the-barrier distances for electron transfer are obtained from the (sequential) conditions that the maxima of the potential barriers equal the corresponding Stark-shifted electronic binding energies $I_r+(q-r+1)/R$, expressed in terms of the distance, R, between the projectile and the (model) sphere center. We calculate R_r numerically and the results are shown in Fig. 5 for r ranging from $r=1$ to

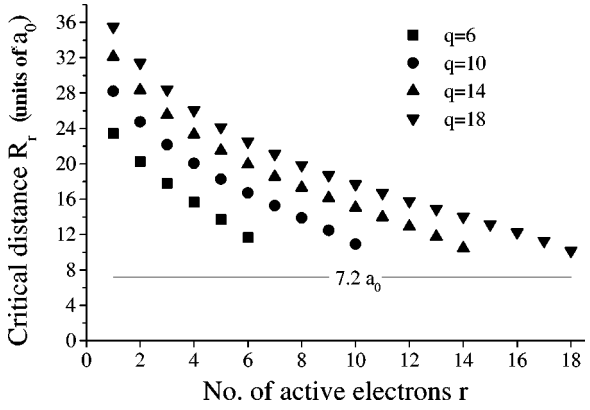

FIG. 5. Critical electron transfer distances, R_r, as functions of the number of active electrons, r, calculated by means of the over-the-barrier concept combined with a metal sphere model of the C_{60} molecule (cf. text). Results for different values of q are shown for $Ar^{q+}-C_{60}$ collisions.

$r=q$ using full screening of the projectile charge [5]. The smallest critical distances correspond to full neutralization ($r=q$) and they lie a few atomic units ($3-4a_0$) outside the sphere radius $a=7.2a_0$.

The model Q value [5] for transfer of r electrons to a projectile of charge q is

$$Q_{\rm tot}^r=\sum_{k=1}^{r}(T_B^{(k)}-I_k), \tag{5}$$

where the individual terms in the sum are [5]

$$T_B^{(k)}=\frac{q-k+1}{R_k}+\frac{a(q-k+1/2)}{R_k^2-a^2}-\frac{a(q-k+1/2)}{R_k^2}+I_k. \tag{6}$$

Note that these expressions for $T_B^{(k)}$ do not directly give the individual binding energies after capture of r electrons. The reason for this is that electrons that become active at smaller R are transferred to more deeply bound projectile states. The binding energies of the outer (already transferred) electrons will then be reduced due to an increased screening of the projectile charge, and the binding energies, $E_B^{(k)}$, will depend on both k and r ($k\leqslant r$). However, the $Q_{\rm tot}^r$ values are well-defined model quantities given by the R_r sequences.

The binding energy of the outermost electron is first calculated through $n_{\rm eff}^{(1)}=q/\sqrt{2E_B^{(1)}}$ for the case in which this is the only transferred electron, for which $E_B^{(1)}=T_B^{(1)}$. For collisions in which two electrons are transferred we assume that the binding energy for the first (outer) one decreases in proportion to the reduced screening, i.e., with a factor $[(q-1)/q]^2$, and, thus, that the value of $n_{\rm eff}^{(1)}$ is unchanged. The binding energy of the second electron then becomes $E_B^{(2)}=T_B^{(2)}+\{1-[(q-1)/q]^2\}T_B^{(1)}$ with $T_B^{(1)}$ and $T_B^{(2)}$ from Eq. (6) giving $n_{\rm eff}^{(2)}=q/\sqrt{2E_B^{(2)}}$. Continuing with this method, we increase the screening for all outer electrons by one unit when a new inner electron is transferred in a stepwise manner. For each step, we calculate the binding energy of the last transferred electron under the condition that the total electronic binding energy, and thus the $Q_{\rm tot}^r$ value given by Eq. (5), is unchanged. The outermost electron in $Ar^{6+}-C_{60}$ collisions will then, e.g., populate $n_{\rm eff}^{(1)}=6.1$ regardless of the total number of transferred electrons r. In Fig. 6, we show $1/(n_{\rm eff}^{(k)})^2$ as functions of k ($k\leqslant r$) for different q. The excitation energy for the last captured electron in close collisions ($k=r=q$) is in most cases sufficient to allow for emission of all the outer $r-1$ electrons for Ar^{q+} projectiles with L holes. This situation contrasts the one for projectiles without L holes as, e.g., Ar^{6+}, where the last two electrons, according to the model, are likely to be captured directly in the M shell (cf. Fig. 6).

B. The decay of hollow ions/atoms

The relative probabilities to *stabilize* $s=1$, 2, 3, or 4 electrons on an argon projectile ion are found to be only very weakly dependent on q (cf. Fig. 3). In the left part of Fig. 7, we show the calculated relative distributions among the cross sections for ionizing the target up to $r=12$. These are based on the critical radii R_r (from Fig. 5) with r ranging from $r=1$ to $r=q-1$. In the right part of Fig. 7, we show a comparison between the model distribution for Ar^{8+}, which does not include processes leading to very strong target ionization ($r\geqslant q$), and measurements from Chen *et al.* [33] including such processes. Strong target ionization is of great principal importance, but normally it only accounts for 10–20 % of the total electron capture cross section. The experimental result by Chen *et al.* [33] for the fraction of processes yielding $r\geqslant q$ is about 10% for $Ar^{8+}-C_{60}$ collisions. This is slightly smaller than the corresponding model value $(R_8/R_1)^2$, which gives 16%.

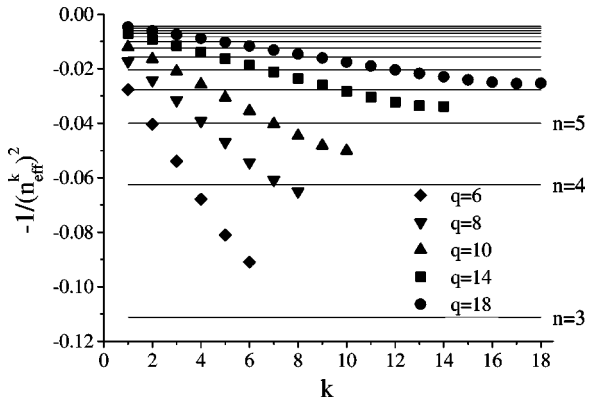

FIG. 6. Model effective quantum numbers, displayed as $1/(n_{\rm eff}^k)^2$ as functions of $k\leqslant r$ for different projectile charge states q. The positions of the hydrogenic quantum numbers, n, are shown to the right in the figure.

From the comparison to the right in Fig. 7 we conclude that the present model gives fair relative r distribution for $r<q$. The close agreement between the calculated distributions in the left figure shows that the weak q dependence in $f_{q,\rm low}^s$ and $f_{q,\rm high}^s$ for $s\leqslant 4$ is manifested already in the corresponding initial electron transfer processes and that this effect somehow is conserved in the subsequent stabilization

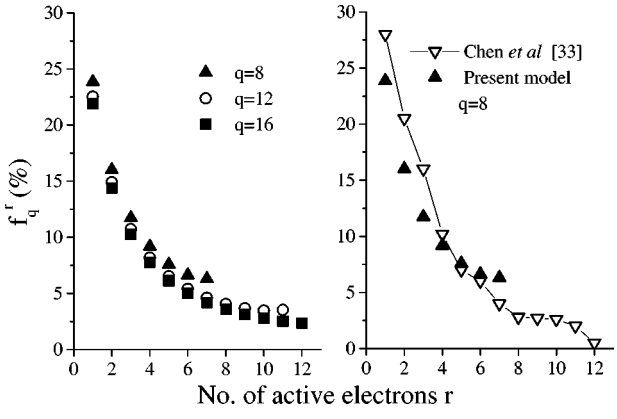

FIG. 7. Left: Relative model ionization cross sections f_q^r for projectile charge states $q=8$, 12, and 16 colliding with C_{60}. Right: Relative target ionization cross sections, f_q^r, from the model and experimental values f_q^r from Chen *et al.* [33] for Ar^{8+}-C_{60} collisions.

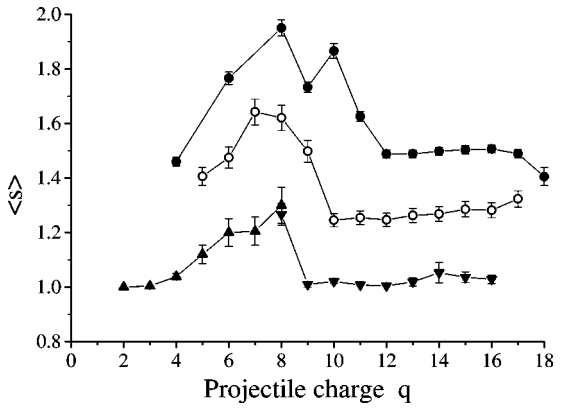

FIG. 8. The mean numbers of stabilized electrons $\langle s \rangle$ as functions of the projectile charge states, q, for Ar^{q+} ions colliding with C_{60} (present data, filled circles), Ar (from [25], open circles), and He [from [26] for $q \leqslant 8$ (filled triangles) and from [27] (filled inverted triangles) for $q \geqslant 8$]. The collision velocities were 0.2, 0.6, and 0.2 a.u. for the C_{60}, Ar, and He targets, respectively.

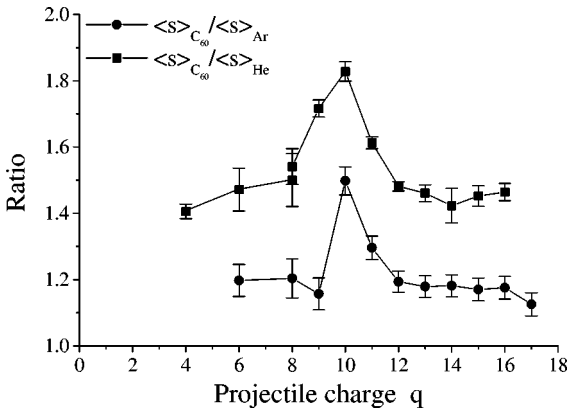

FIG. 9. The ratios between the number of electrons stabilized on Ar^{q+} projectiles following collisions with C_{60} and atomic targets; $\langle s \rangle_{C60}/\langle s \rangle_{Ar}$ (filled circles) and $\langle s \rangle_{C60}/\langle s \rangle_{He}$ (filled square). The values for $\langle s \rangle_{Ar}$ and $\langle s \rangle_{He}$ are taken from Refs. [25] and [26,27], respectively.

process. A possible way to understand this is if the number of stabilized electrons is determined directly by the relative r distributions (which are weakly dependent on q) rather than by the projectile charge itself. In other words, it appears as if electric charge is dissipated in similar ways independent of the core structure and that the dominant autoionization processes thus mainly involve higher excited states for $s \leqslant 4$.

C. Comparisons with ion-atom collisions

In Fig. 8, we show the mean numbers of electrons stabilized on the Ar^{q+} projectile together with similar results for Ar^{q+}-Ar [25] and Ar^{q+}-He [26,27] collisions. The three sets of data in Fig. 8 show important differences and similarities. They reach their respective (almost) constant high-q values of $\langle s \rangle = 1.5$, 1.3, and 1.03 at $q = 12$, 10, and 9 for the C_{60}, Ar, and He targets, respectively. The most striking observations are the maxima in $\langle s \rangle$ around $q = 8$ for all three targets and the unique second maximum at $q = 10$ for C_{60}. The collision velocity was higher for the Ar target (0.6 a.u. [25]) than for the C_{60} (0.2 a.u.) and the He targets (0.2 a.u. [26,27]), but in the low-velocity regime ($v < 1$ a.u.) this is of minor importance.

The mean numbers of stabilized electrons for the two-electron target He, $\langle s \rangle_{He}$, are only slightly larger than unity for $q \geqslant 9$ (cf. Fig. 8). The higher values of $\langle s \rangle_{He}$ for lower q ($q = 5-8$) are due to direct population of the M shell by the inner of the two transferred electrons as described by, e.g., Selberg *et al.* [34]. For $q \leqslant 8$, the projectile L shells are completely filled and autoionization is suppressed. In fact, $\langle s \rangle_{He} = 1.3$ is equal to the expected maximum value for $q = 8$ with zero autoinization rate and a relative two-electron transfer probability of 0.3. The latter was suggested by experiments in which the relative yields of He^{2+} and He^{+} recoil ions were measured to be close to 0.3 independent of the projectile charge [35]. Note also that the number of stabilized electrons is always larger for Ar^{q+}-Ar than for Ar^{q+}-He collisions (Fig. 8). Qualitatively, this is easy to understand, since more than two electrons may be transferred from argon. Therefore, it is still possible, after first filling one L-shell vacancy in an Auger process, to stabilize one (or several) of the remaining excited electrons by further Auger and/or radiative processes. We interpret the maximum at $q = 8$ for the C_{60} target as due to similar processes to those for the atomic targets, i.e., direct over-the-barrier (''side-feeding'') of the argon M shell. This is supported by the calculated sequences of projectile capture states (cf. Fig. 6) and by the comparison with the O^{8+}-C_{60} results from Chen *et al.* [33]. The O^{8+} projectile has empty K and L shells and therefore the cross sections, σ_q^s, for large s are much smaller than for Ar^{8+} projectiles.

The second maximum in $\langle s \rangle$, at $q = 10$, is unique for the Ar^{q+}-C_{60} collision system and indicates that the L shell somehow is efficiently filled for Ar^{10+} but not for Ar^{q+} projectiles with $q \geqslant 12$. This is clearly exposed in Fig. 9, where the ratios $\langle s \rangle_{C60}/\langle s \rangle_{Ar}$ and $\langle s \rangle_{C60}/\langle s \rangle_{He}$ are shown. So far, we have assumed that electrons are transferred sequentially from the *outermost* C_{60}^{r+} orbitals such that the last transferred inner electrons reach the M shell for $q \leqslant 8$. This, however, could not explain direct population of the Ar L shell due to the large difference between the tenth ionization potential of C_{60} (42 eV) and the L-shell energy of Ar^{10+} (479 eV). Instead, the second maximum at $q = 10$ is most likely due to resonant, over-the-barrier transfer to argon L holes of one (or two) carbon K-shell electrons (the K-shell energies are 290 eV [36] and 292 eV [37] for neutral C_{60} and atomic carbon, respectively). The Stark shift plays an important role here and, as an example, an unscreened $q = 10$ projectile charge would shift the carbon K energy to 479 eV at a separation of $R = 10 \times 27.2/(479-290) = 1.4a_0$.

Electron transfer between the carbon K and the argon L shells has been observed for ion-*atom* collisions by deNijs *et al.* [22]. They recorded strongly enhanced production of Ar^{7+} and Ar^{8+} recoil ions in C^{6+}-Ar collisions. A rather detailed analysis of projectile and target Stark shifts and the mutual screening led to the conclusion that the effective K-L transfer distances are around $1.5a_0$ [22]. This value is close to our rough estimate, and the fraction of the total electron-

capture cross section involving *K*-shell capture could thus be estimated to be $[(7.2+1.5)/29]^2=0.1$ with $R_1=29a_0$ being the first critical distance for $q=10$. Although this effect is sufficiently large to qualitatively explain the enhanced value of $\langle s\rangle_{C60}$ for $q=10$ (Figs. 8 and 9), we still have to understand why there is no enhancement for $q\geqslant 12$. The most likely explanation is, we believe, that the *K* electrons are transferred to the *M* and not to the *L* shell for these higher charges and that they thus leave holes in the *L* states even after carbon *K*-shell capture. The binding energies for the $3s$ states to Ar^{q+} with $q=10$, 11, 12, 13, and 14 are 196, 227, 257, 297, and 326 eV, respectively [37]. Comparing these values with the 292 eV C_{60} *K* shell energy [36], it appears reasonable to assume that the latter three lead to transfer to the *M* shell at distances larger than those where direct transfer to the *L* shell would be effective.

Very efficient carbon *K*-shell vacancy production has recently been observed in carbon atoms sputtered by highly charged ions from graphite and C_{60}-covered surfaces [38].

D. Comparisons with ion-surface interactions

The basic mechanism behind the enhanced stabilization for low *q* is direct over-the-barrier transfer to the *M* shell of argon at distances of a few atomic units outside the C_{60} cage. Similar processes are discussed by Winecki *et al.* [16,17] in order to explain neutralization of slow Ar^{q+} ions after grazing reflections above a graphite surface. The neutralization probability was shown to be close to 1 and independent of *q*. Winecki *et al.* [16,17] argued that the efficient neutralization processes of projectiles with *L*- and *K*-shell vacancies were due to decay processes sufficiently fast to allow repeated filling of the *M* shell during the close (above-surface) interaction with graphite. That is, fast sequences of (mainly) *LMM* Auger decays are supported by continuing resonant over-the-barrier transfers to the *M* shell. The relevant Auger lifetimes are sensitive to the number of electrons in the *L* and *M* shells, n_L and n_M, through the expression (see [17] and references therein)

$$\tau=\frac{250\times 10^{-15}}{(8-n_L)n_M(n_M-1)}\ \text{s} \tag{7}$$

for $n_M\geqslant 2$. A key point is that all projectiles interact closely with the flat surface during fairly large parts of their trajectories and for fairly long times, of the order of 10 fs. In contrast, a C_{60} molecule has a curved surface and the projectiles will only occasionally come close enough for direct over-the-barrier transfer to the *M* shell. Even then, trajectories are typically only sufficiently close during times of the order of a few tenths of a femtosecond. With, e.g., a half-filled *L* shell, τ ranges from $\tau=30$ down to $\tau=1$ fs when the number of electrons in the *M*-shell increases from $n_M=2$ to $n_M=8$. Thus, the time-bottleneck limitation prevents efficient filling of the projectile inner shells from C_{60}. Still, we know from the measurements of Martin *et al.* [21] that large amounts of electrons are emitted during very brief interactions between highly charged ions and C_{60}.

Here, we argue that strong electron emission from C_{60}, in the absence of efficient projectile neutralization, may be qualitatively explained in the following way: The projectiles are neutralized on the incoming trajectory, and according to the simple model discussed here, the last of the *q* active electrons transfers at a distance of $3-4a_0$ above the C_{60} surface for all *q* (see Fig. 5). For high *q*, several intermediate shells are left empty ($n_{\text{eff}}^{(18)}\approx 6$ in Fig. 6), and if the projectile charge, e.g., $q=18$, is not fully screened by the 18 active electrons, electron transfer will continue as the projectile approaches. As a consequence, the outer electrons in the hollow atom will be dissipated on a very short time scale as they no longer experience a positive effective projectile core charge.

V. CONCLUSIONS

We have investigated electron transfer and stabilization in slow Ar^{q+}-C_{60} collisions for projectiles with charge states ranging from $q=4$ to $q=18$. For large impact parameters, the picture is the following: As the projectile approaches the C_{60} target, electrons transfer sequentially from the *outermost* molecular target orbital to the projectile. This may be described as over-the-barrier processes, and the number of transferred electrons, *r*, is given by the projectile charge and the impact parameter. The hollow ions/atoms that are formed in this way decay (mainly) after the collision and leave one or, at most, a few electrons, *s*, stabilized on the projectile. These processes typically account for more than 80% of the total electron-capture cross section, and we conclude that Ar^{q+}-C_{60} collisions are dominated by atomlike behavior. Experimentally, we find that the relative distributions on *s* only depend very weakly on *q* for $s\leqslant 4$. That is, the relative probabilities for $s=1$, 2, 3, or 4 are not strongly dependent on the number of projectile *K*-, *L*-, and *M*-shell vacancies.

For small impact parameter Ar^{q+}-C_{60} collisions, the picture becomes more complex: Sequential, over-the-barrier electron transfer from the outermost C_{60}-target orbitals proceeds along the approaching trajectory. In our model, we find that full initial neutralization for all *q* is reached at distances $3-4a_0$ above the C_{60} cage, thus completing the initial hollow atom formation. The sequence of effective quantum numbers for the six electrons initially neutralizing, e.g., Ar^{6+} ranges from $n_{\text{eff}}^{(1)}=6.1$ for the outermost to $n_{\text{eff}}^{(6)}=3.1$ for the innermost one. In contrast, the effective quantum states for, e.g., Ar^{14+} with six *L* vacancies ranges from $n_{\text{eff}}^{(1)}=11$ to $n_{\text{eff}}^{(14)}=5.5$. Thus, direct population of the *M* shell seems to occur only for argon projectiles without *L* holes as supported by similar increased stabilization probabilities for Ar^{q+}-Ar [25] and Ar^{q+}-He [26,27] collisions with $q\leqslant 8$. A surprising enhancement in stabilization is observed also for Ar^{10+}- and Ar^{11+}-C_{60} collisions. This effect is due to energy resonances between the carbon *K* and the argon *L* shells at Ar-C distances around one atomic unit in a similar way to that observed by deNijs *et al.* for C^{6+}-Ar collisions [22]. For $q\geqslant 12$, however, the carbon *K*-shell energies become resonant with the argon *M* shells at distances that are larger than those for *L*-shell transfer and thus the latter are blocked, giving lower and nearly constant stabilization probabilities for high *q*.

We have shown that the interaction times within close distances in general are too short (subfemtoseconds) to allow side-feeding and Auger decay to fill inner-shell vacancies from C_{60} in the same way as from, e.g., a graphite surface. Still, in spite of this limited time and the surviving inner-shell holes, the filling of intermediate shells of *hollow atoms* offers a qualitative picture of how outer electrons may be effectively dissipated through screening of the projectile charge. We believe that this is the main cause for strong electron emission in close interactions between highly charged ions and C_{60}.

ACKNOWLEDGMENTS

This work was supported by the Swedish Natural Science Research Council under Contract No. F-AA/FU 08801-325 and F 5102-993/1999, and by the Swedish Foundation for International Cooperation in Research and Higher Education (STINT) at the Manne Siegbahn Laboratory. We are grateful to M. Björkhage and L. Liljeby for preparing the ion beam and to P. Hvelplund at Aarhus University for discussions of the results.

[1] R. Morgenstern, T. Schlathölter, and R. Hoekstra, in *Proceedings of the XXI International Conference on the Physics of Electronic and Atomic Collisions (ICPEAC), Sendai, Japan 1999*, AIP Conf. Proc. No. 500, edited by Y. Itikawa, K. Okuno, H. Tanaka, A. Yagishita, and M. Matsuzawa (AIP, Melville, NY, 2000).
[2] H. Cederquist, A. Fardi, K. Haghighat, A. Langereis, H. T. Schmidt, and S. H. Schwartz, Phys. Scr., T **80**, 46 (1999).
[3] B. Walch, C. L. Cocke, R. Voelpel, and E. Salzborn, Phys. Rev. Lett. **72**, 1439 (1994).
[4] U. Thumm, A. Bárány, H. Cederquist, L. Hägg, and C. J. Setterlind, Phys. Rev. A **56**, 4799 (1997).
[5] H. Cederquist, A. Fardi, K. Haghighat, A. Langereis, H. T. Schmidt, S. H. Schwartz, J. C. Levin, I. A. Sellin, H. Lebius, B. Huber, M. O. Larsson, and P. Hvelplund, Phys. Rev. A **61**, 022712 (2000).
[6] S. Ninomiya, Y. Yamazaki, F. Koike, H. Masuda, T. Azuma, K. Komaki, K. Kuroki, and M. Sekiguchi, Phys. Rev. Lett. **78**, 4557 (1997).
[7] K. Tokesi, L. Wirtz, C. Lemell, and J. Burgdörfer, Phys. Rev. A **61**, 020901(R) (2000).
[8] H. Kurz, F. Aumayr, H. P. Winter, D. Schneider, M. A. Briere, and J. W. McDonald, Phys. Rev. A **49**, 4693 (1994).
[9] H. P. Winter and F. Aumayr, J. Phys. B **32**, R39 (1999).
[10] C. Lemell, J. Stöckl, J. Burgdörfer, G. Betz, H. P. Winter, and F. Aumayr, Phys. Rev. Lett. **81**, 1965 (1998).
[11] H. Winter, C. Auth, R. Schuch, and E. Beebe, Phys. Rev. Lett. **71**, 1939 (1993).
[12] F. W. Meyer, L. Folkerts, and S. Schippers, Nucl. Instrum. Methods Phys. Res. B **100**, 366 (1995).
[13] C. Auth and H. Winter, Phys. Lett. A **217**, 119 (1996).
[14] L. Hägg, C. O. Reinhold, and J. Burgdörfer, Phys. Rev. A **55**, 2097 (1997).
[15] J. Burgdörfer and F. Meyer, Phys. Scr. T **T46**, 225 (1993).
[16] S. Winecki, M. Stöckli, and C. L. Cocke, Phys. Rev. A **56**, 538 (1997).
[17] S. Winecki, C. L. Cocke, D. Fry, and M. P. Stöckli, Phys. Rev. A **53**, 4228 (1996).
[18] S. Winecki, M. P. Stöckli, and C. L. Cocke, Phys. Rev. A **55**, 4310 (1997).
[19] L. Folkerts and R. Morgenstern, Europhys. Lett. **13**, 377 (1990).
[20] S. H. Schwartz, A. Fardi, K. Haghighat, A. Langereis, H. T. Schmidt, and H. Cederquist, Phys. Rev. A **63**, 013201 (2000).
[21] S. Martin, L. Chen, A. Denis, and J. Désesquelles, Phys. Rev. A **59**, R1734 (1999).
[22] G. de Nijs, H. O. Folkerts, R. Hoekstra, and R. Morgenstern, J. Phys. B **29**, 85 (1996).
[23] J. Abrefah, D. R. Olander, M. Balooch, and W. J. Siekhaus, Appl. Phys. Lett. **60**, 1313 (1992).
[24] M. O. Larsson, P. Hvelplund, M. C. Larsen, H. Shen, H. Cederquist, and H. T. Schmidt, Int. J. Mass Spectrom. Ion Processes **177**, 51 (1998).
[25] R. Ali, C. L. Cocke, M. L. A. Raphaelian, and M. P. Stöckli, Phys. Rev. A **49**, 3586 (1994).
[26] A. Müller and E. Salzborn, Phys. Lett. **59A**, 19 (1976).
[27] J. Vancura, V. J. Marchetti, J. J. Perotti, and V. O. Kostroun, Phys. Rev. A **47**, 3758 (1993).
[28] A. Bárány and C. J. Setterlind, Nucl. Instrum. Methods Phys. Res. B **98**, 184 (1995).
[29] H. Steger, J. Holzapfel, H. Hielscher, W. Kamke, and I. V. Hertel, Chem. Phys. Lett. **234**, 455 (1995).
[30] M. Sai Baba, T. S. Lashkimi Narashimhan, R. Balasubramanian, and C. K. Mathews, Int. J. Mass Spectrom. Ion Processes **125**, R1 (1993).
[31] C. Lifshitz, M. Iraqi, T. Peres, and J. E. Fischer, Rapid Commun. Mass Spectrom. **5**, 238 (1991).
[32] R. Antoine, Ph. Dogourd, D. Rayane, E. Benichou, M. Broyer, F. Chandezon, and C. Guet, J. Chem. Phys. **110**, 9771 (1999).
[33] L. Chen, J. Bernard, A. Denis, S. Martin, and J. Dësesquelles, Phys. Scr. T **T80**, 52 (1999).
[34] N. Selberg, C. Biedermann, and H. Cederquist, Phys. Rev. A **56**, 4623 (1997).
[35] H. Cederquist, E. Beebe, C. Biedermann, Å. Engström, H. Gao, R. Hutton, J. C. Levin, L. Liljeby, T. Quinteros, N. Selberg, and P. Sigray, J. Phys. B **25**, L69 (1992).
[36] S. Aksela, E. Nommiste, J. Jauhiainen, E. Kukk, J. Karvonen, H. G. Berry, S. L. Sorensen, and H. Aksela, Phys. Rev. Lett. **75**, 2112 (1995).
[37] S. Bashkin and J. O. Stoner, Jr., *Atomic Energy Levels and Grotrian Diagrams* (North Holland, Amsterdam, 1975), Vol. II.
[38] T. Schlathölter, A. Närmann, A. Robin, D. F. A. Winters, S. Marini, R. Morgenstern, and R. Hoekstra, Phys. Rev. A **62**, 042901 (2000).